

ACOUSTIC TEXTURES AND MULTIBEAM MAPPING OF SHALLOW MARINE HABITATS – EXAMPLES FROM EASTERN MALTA

Ph Blondel Department of Physics, University of Bath, UK
M Prampolini Department of Chemical and Geological Sciences, Università degli Studi di Modena and Reggio Emilia, Modena, Italy
F Fogliani Istituto di Scienze Marine, CNR-ISMAR, Bologna (Italy)

1 INTRODUCTION

Habitat mapping is expanding into deeper waters, for which existing tools like sidescan sonars and Multibeam Echo-Sounders (MBES) are already tried and tested, to increasingly shallower waters. The adaptation of systems designed for deeper waters to more restricted ranges, often with multiple reflections, and more varied seabeds, often with overlaying vegetation or habitats, has been associated with significant technological challenges. The resulting step change in acoustic mapping has brought much higher spatial resolutions, at least an order of magnitude better, but also a higher variability to small-scale variations and survey settings. Maps of marine habitats have several purposes, from ecological (ecosystem health monitoring, marine-protected areas) to socio-economic (resource accessibility and sustainability, changes brought by land-based processes, pollution or offshore activities). Classifications must therefore successfully address the relevant types of information.

A large part of these classification activities relies on similar techniques, looking at variations in backscatter (in particular textures) and/or bathymetry to identify seabed and habitat types^{1,2,3,4,5}. Previous studies have shown that interpretation could be affected by large-scale slopes not accounted for during processing⁶ or by changes in survey speed/sonar depth⁷. These changes may affect subsequent classifications and interpretations, and the present study aims at presenting the results of acoustic texture analyses in the context of data acquisition choices (e.g. pulse lengths, survey speeds), terrain morphology (role of slopes and large-scale types) and multi-scale terrain variability (bathymetry and backscatter), using a typical MBES map of a complex, shallow-water area offshore Eastern Malta.

2 MULTIBEAM HABITAT MAP

The acoustic measurements presented here are part of a larger dataset, acquired along the Eastern coast of Malta in May 2012, in water depths varying between 1.5 and 290 m^{4,8}. The Kongsberg EM710 multibeam echosounder (MBES) installed on board R/V *Urania* mapped the seafloor of the Maltese archipelago, from north of Gozo to SE Malta, using 258 equidistant beams of 1° by 1°. Bathymetry and surface backscatter were processed with Caris HIPS and SIPS, producing a Digital Elevation Model and an imagery dataset with final resolutions of 2 metres, for an entire area of 1,390 km².

The present work focuses on a section of 4.4 x 3 km north of Gozo Island, offshore Marsalforn Bay (Figure 1). Depths range between 13 m and 215 m, following the present coastline and with escarpments parallel to it. The area is bordered seaward by three breaks of slope at the respective depths of 75, 110 and 132 m, marking the transition from the shelf to the surrounding Malta Plateau. The central structure is the SW-NE channel of a palaeo-river, with steep slopes. Red boxes highlight areas where grab samples give more information about the geology and habitats. Morphological structures include horst and graben alternations, seagrass cover (*Posidonia oceanica* and *Cymodocea nodosa*) in some areas, maërl and different sediment types, including

karst, bedrock, patches of fine or medium sand, and alternation of sand and gravel with blocks of calcarenite (5-20 cm in size, from one of the grab samples).

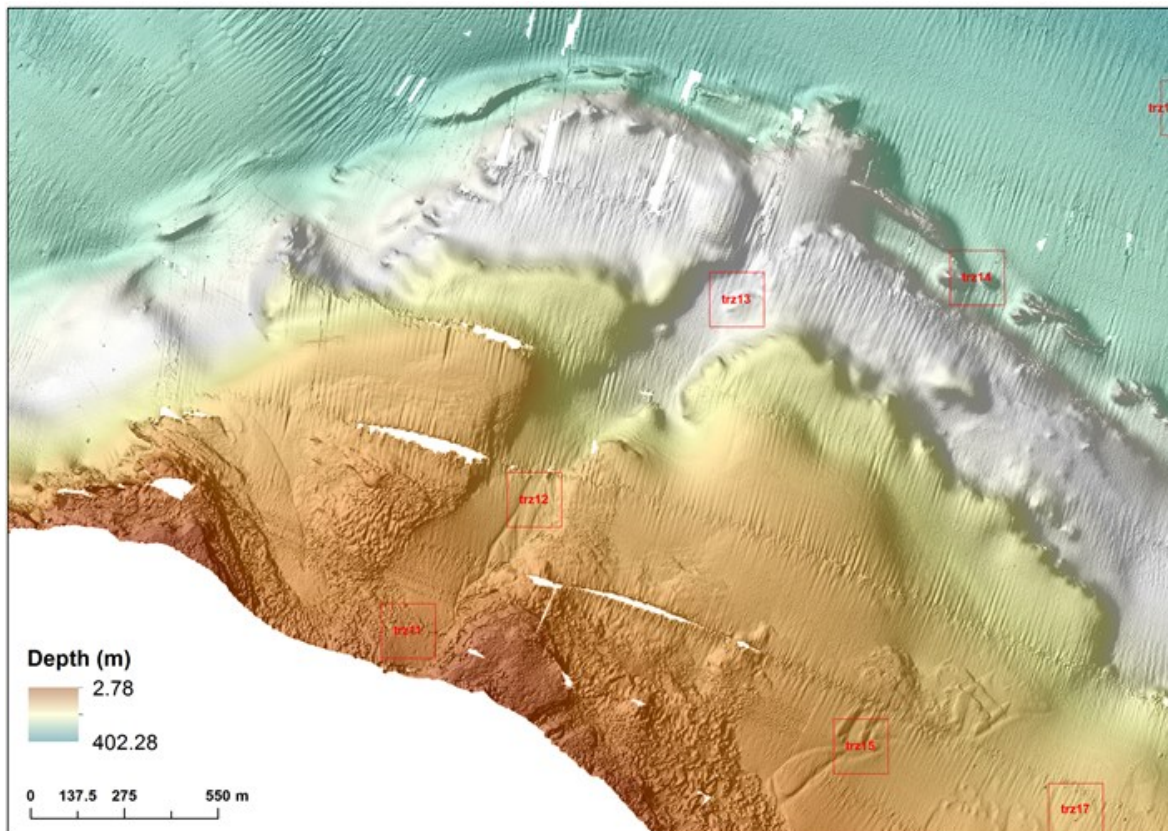


Figure 1. MBES bathymetry from the study area. The colour scale has been expanded to highlight the different geomorphological regions (actual depths vary between approx. 15 and 250 m). The key structures are the shallow slopes continuing from the island, with clear breaks following the palaeo-shorelines down to the Malta Plateau, and the incised palaeo-channel (wied) incising the slope from SW to NE. Red boxes indicate Training Zones for which grab samples were available.

Surface backscatter intensities processed at the same resolution (Figure 2) range from close to 0 dB (white) down to -71.2 dB (black). The higher values are located on the continental shelf, whereas the lower values are associated with the slope/basin area. A secondary channel, sub-perpendicular to the large palaeo-channel visible in the bathymetry and in the backscatter, is also revealed, with very small slopes.

3 ACOUSTIC TEXTURES

Sonar imagery represents backscatter for individual pixels, averaging acoustic returns for small square areas (2-m long in this study). Backscatter is affected by the local geometry of the seabed (slopes facing toward the imaging sonar will reflect more energy than slopes facing away); the type of seabed (rocky outcrops scattering more energy than sediments, for example); the micro-scale roughness at scales comparable to the imaging wavelength, approx. 2 cm in this study (rougher terrains scattering more at all directions than smoother terrains, for which specular returns are higher) and the relative contributions of surface and volume scattering (dependent on seafloor types but also on factors such as the amount of bioturbation). In shallower areas, the presence of vegetation or other habitats (e.g. maerl, Coralline red algae) will also affect these individual acoustic

returns. Modern sonar systems can also vary the pulse length (0.2 to 2 ms in this study), which affects the size of the scattering area/volume.

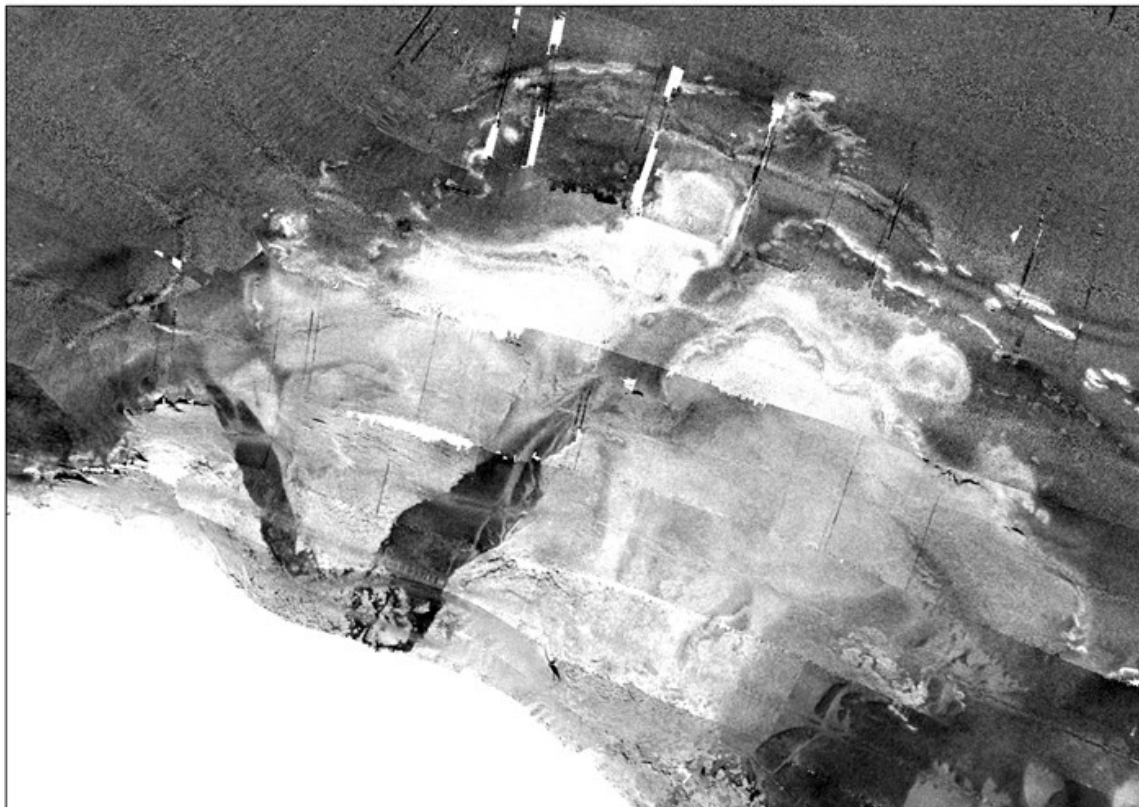


Figure 2. Backscatter imagery corresponding to Figure 1, at the same resolution of 2 m.

Interpretation of the sonar imagery relies on the mean and deviation of the average levels in larger groups, at scales comparable to expected features (e.g. 20 m, or 10 pixels, for individual, small outcrops, or 100 m, i.e. 50 pixels, for larger structures or sediment patches). These first-order statistics are generally supplemented by the textural patterns typical of different terrain types, and second-order statistics have proved the most adapted to different types of sonar imagery (e.g. sidescan⁹ and MBES^{3,10}). The *TexAn* suite has been used for a large variety of studies, mapping geological units¹¹, identifying small targets on complex backgrounds¹², quantifying distributions of habitat types^{9,10} and comparing information from MBES bathymetry and imagery with selective ROV video information^{3,5,10}. *TexAn* groups individual pixels into moving square windows of a specific size (WD pixels), calculating Grey-Level Co-occurrence Matrices (GLCMs) over a specific number NG of grey levels, for pixels at a distance SZ from each other, averaging them over all orientations and deriving statistical measures, called textural indices, for each point. The mathematical details are given in the preceding articles and need not be repeated here. Two indices, entropy and homogeneity, were found to be the most adapted in distinguishing terrain types and detecting unexpected targets. Moreover, because second-order statistics are able to detect subtle changes invisible to the human eye, they can provide additional information for human or computer-assisted interpretation.

TexAn first converts the original image (with a 71.2 dB backscatter range) to 8 bits (256 grey levels), resulting in a dynamic range of 0.28 dB per grey level. Square Training Zones approximately 80-pixels wide are selected on the basis of prior information or available ground truth. For this dataset, 20 Training Zones were used, supplemented with grab samples, and 7 of these Training Zones overlap with the area of Figures 1 and 2. Entropy and homogeneity were calculated for each pixel in these Training Zones, varying grey levels from NG = 8 to NG = 256 by factors of 2,

window sizes from $WD = 10$ pixels to $WD = 60$ pixels by increments of 10 pixels, and inter-pixel separations by $SZ = 5$ pixels to $WD - 5$ pixels by increments of 5 pixels. The optimal combination (out of 1,296 possible cases) was assessed on the separation between Training Zones, and it corresponds to $NG = 64$ grey levels (i.e. looking at differences of approx. 1.1 dB), $WD = 50$ pixels and $SZ = 5$ pixels (i.e. looking at scales of 10 m, but within 100-m ranges). Entropy and homogeneity were therefore computed with these values for the entire dataset (Figure 3), and their clustering (with K-Means) was validated with local geology and other interpretations^{4,8} to yield the final classifications. The progression in entropy and homogeneity is associated with increasing grain sizes. The more sedimented or homogeneous areas have lower entropies and homogeneities (e.g. “fine sand”). Both textural signatures increase for coarse sand (slightly rougher but less homogenised), medium sand and gravel/blocks (rougher textures at this scale, with local organisation visible at scales less than 60 m).

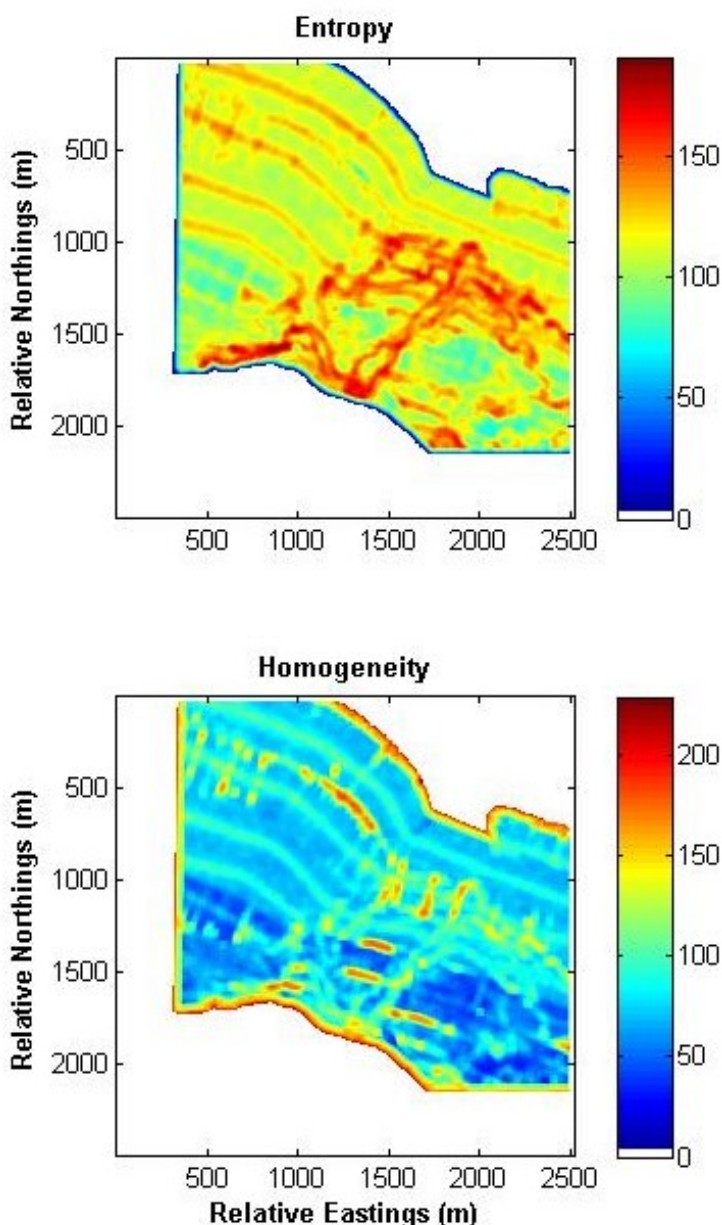


Figure 3. Acoustic textures computed for the backscatter imagery of Figure 2 after identification of the optimal parameters to distinguish a large number of training zones in the larger dataset.

4 SURVEY AND SEABED INFLUENCES

The area studied (Figure 1) shows a large variation of terrains, depths, slopes and backscatter levels. The survey itself was made of several lines followed at varying speeds, depending on weather conditions and other considerations, and used different pulse lengths. Did any of these variations affect acoustic textures, and if so, does it need accounting for in the calculations and/or the interpretations of specific regions?

Local bathymetry and backscatter were processed at the same 2-m resolution, similar to entropy and homogeneity values. Local slopes, derived with ArcGIS 10.1 from the maximum rate of change in bathymetry from the central pixel to its 8 immediate neighbours, correspond to distances of 6 m on the ground and are calculated at the same 2-m resolution. Entropy and homogeneity were calculated on square windows of size $WD = 50$ pixels, looking at variations between pixels $SZ = 5$ pixels away from each other. Averages and standard deviations of the other values are therefore calculated on square windows of sizes increasing from 5 pixels wide to the entire size of the computation window.

Bathymetry averages correspond to the local depth in the area over which textures are calculated. They show weak correlations with entropy (-0.4 to -0.52) and with homogeneity (-0.43 to -0.57), becoming slightly more anti-correlated as they are assimilated over large windows. Entropy is poorly correlated with bathymetric roughness (0.37 - 0.41), increasing as more pixels are accounted for, but it is still not really significant. Homogeneity is less correlated (0.32 to 0.36). These results are expected, as textures are defined on the basis of backscatter variations.

Local slopes span the entire range from 0° to 87° (Figure 4), with the larger values corresponding to breaks between geomorphological regions. Entropy shows weak correlations (0.40 to 0.46), increasing slightly as the slopes are calculated over ranges similar to the size of the texture computation window, and homogeneity shows similarly small correlations (0.35 – 0.39). Similar values are found for the correlation with the variations in slopes: 0.35 – 0.44 for entropy, increasing with the area over which they are calculated, and 0.38 – 0.42 for homogeneity, peaking around half the size of the texture computation window. These low values mean that local slopes, at scales from 6 to 150 m, do not affect the values of textures, despite their large variations throughout the dataset. This is a likely indication that variations of backscatter with angles of imaging by the MBES were adequately processed with CARIS, even though backscatter would have varied with slopes because of the different geological processes and habitats.

Conversely, both entropy and homogeneity show high correlations with the average backscatter (respectively -0.7 to -0.8 and -0.6 to -0.7 as window sizes increase) and with variations in backscatter (0.7 to 0.8 for both). The correlation of entropy with the variations in backscatter increases sharply with window size, which is expected as it is associated to the roughness of the local texture. Homogeneity is associated with the amount of organisation within the local texture, increasing sharply until half the size of the texture computation window and decreasing beyond (presumably as organisation is less easy to detect and quantify for windows larger than WD).

As multibeam swaths are acquired, variations in survey speeds might introduce gaps between swaths (if the ping rate is not adapted) or oversample some areas. Analyses of survey speeds showed they were extremely low and within the same ranges, ensuring even coverage of the seabed at scales below the final, processed resolution and at locally constant velocities. Pulse lengths were unfortunately not logged during operation, but were expected to increase with depth below the surveying vessel. Manufacturer's data shows they are varying between 0.2 and 2 ms. As a crude approximation, the bathymetry distribution was used to divide the survey area into four domains: deeper than -186 m; between -186 and -118 m; between -118 and -81 m and shallower than -81 m. No variation of acoustic textures with these domains could be found that could not be associated with the geological variations of the seabed.

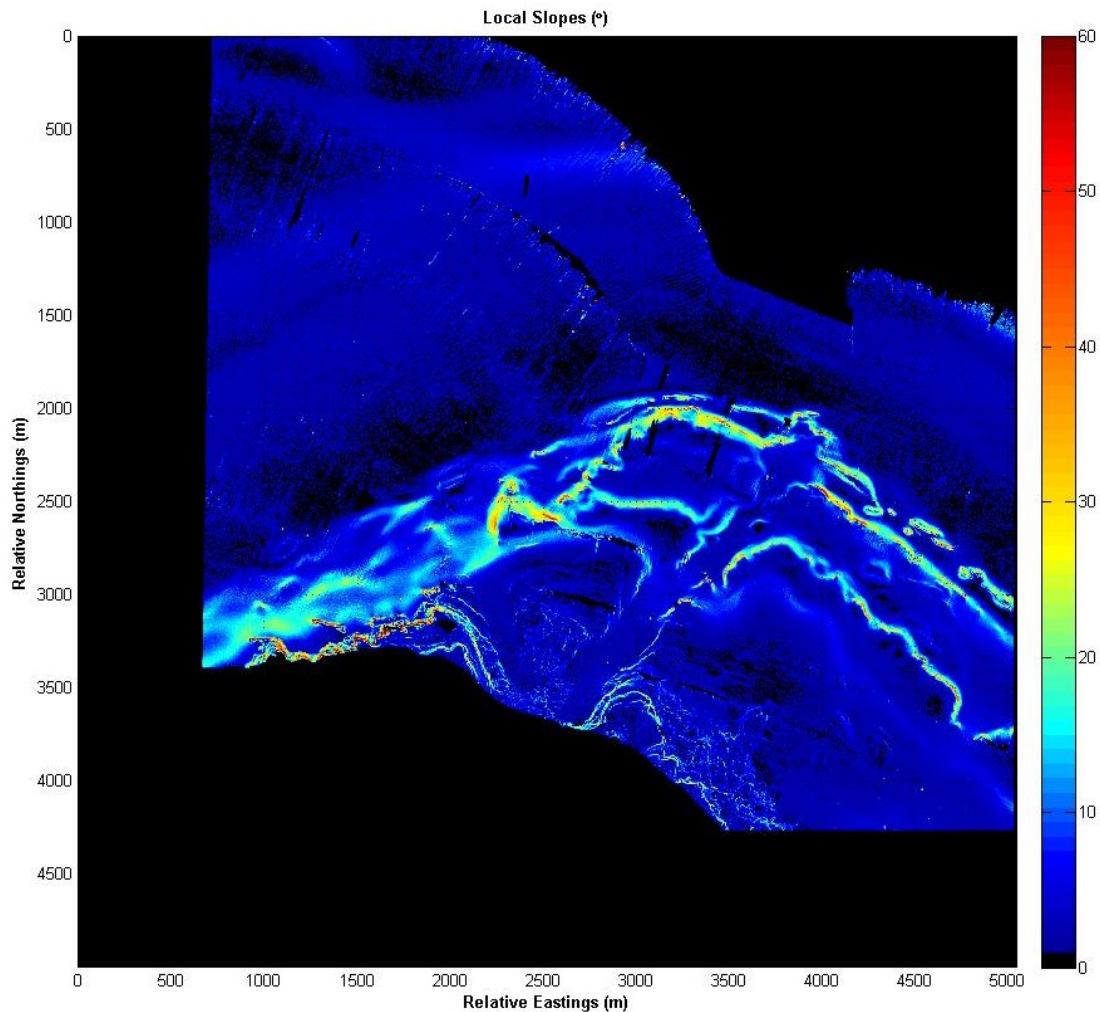


Figure 4. Slopes (calculated on 3x3 neighbourhoods) show the highest values for the breaks between geomorphological regions, and are mostly lower than 10° over ranges of 6 m (3 pixels at 2-m resolution).

5 CONCLUSIONS

The mapping of marine habitats is currently expanding to more varied habitats, in particular in shallower waters than traditionally surveyed, often with much higher resolutions than previously obtainable. The larger variations in survey and acoustic mapping might be compounded with the larger variations in terrain types, in turn affecting the results of classification techniques used to process and interpret large datasets. This short article aimed at comparing the results of acoustic texture analyses in a known terrain, benefiting from adequate ground truth, with data acquisition choices (e.g. pulse lengths, survey speeds), terrain morphology (role of slopes and large-scale types) and multi-scale terrain variability (bathymetry and backscatter).

Data acquisition choices did not seem to have effects on the acoustic maps or their textural analyses. Survey speeds were rather low throughout the survey, and did not vary very much. Data processing (with CARIS) adequately compensated for the uneven sampling of terrains in slopes and for variations of backscatter with imaging angles. Pulse lengths, although not logged during the survey, were approximated by broad depth regions and were not found to have any influence either. Full recording of pulse lengths during similar surveys should however be analysed to draw more authoritative answers to assess how its variations (if any) might affect the data.

Terrain morphology showed a large variation of depths (from 13 m to 215 m) and local slopes (from 0° to 87°, with the larger values corresponding to breaks between geomorphological regions). Acoustic textures were not affected by these variations, at least at scales commensurate with the areas over which they were calculated. Training Zones were used to optimise the window sizes and inter-pixel distances over which textures were computed. They were selected on the basis of homogeneous geology or habitat type, likely to vary with depths/slopes, and the low correlations of textures with terrain morphology further confirm these distances were adequately chosen and repeatable throughout the survey area.

Multi-scale terrain variability showed much higher correlations of textures with backscatter averages and variations, in line with their definition. Entropy, associated to the roughness of local textures, is increasingly correlated with backscatter variability as they are calculated over similar areas. Homogeneity, associated to the amount of local organisation, is also correlated with backscatter variability at similar scales, generally less than half the size of the computation windows.

In conclusion, this study, performed on a moderately-sized area but over a large number of MBES measurements of bathymetry, backscatter and derived textures (entropy and homogeneity), with low variations in survey settings, did not show any undue effect on classification results.

Acknowledgements: The multibeam imagery and bathymetry presented here were acquired aboard R/V Urania (CNR, Italy), whose officers and crew are gratefully thanked. Part of this study benefited from the presence of MP as an exchange postgraduate student at the University of Bath in 2014.

6 REFERENCES

1. C. Brown and Ph. Blondel., 'Developments in the application of multibeam sonar backscatter data for seafloor habitat mapping', *App. Acous.* 70(10) 1242-1247. (2009).
2. T.P. LeBas, A. Micallef, Ph. Blondel, V.A.I. Huvenne and A. Deidun, The combination of morphological and textural techniques for benthic habitat mapping – a case study from a shallow coastal area with high-resolution multibeam and ROV data, *Proc. GeoHab-2012* (2012).
3. A. Micallef, T.P. LeBas, V.A.I. Huvenne, Ph. Blondel, V. Hühnerbach and A. Deidun., 'A multi-method approach for benthic habitat mapping of shallow coastal areas with high-resolution multibeam data', *Cont. Shelf. Res.* 39-40, 14-26. (2012).
4. M. Prampolini, Ph. Blondel, F. Foglini and M. Soldati, Habitat mapping and acoustic textures on the continental shelf of the Maltese islands, *Proc. EuroGEO, Malta* (2014)
5. G. Montereale Gavazzi, F. Madricardo, M. Sigovini, L. Janowski, A. Kruss, Ph. Blondel and F. Foglini., 'Evaluation of seabed mapping methods for fine-scale benthic habitat classification in extremely shallow environments – Application to the Venice Lagoon, Italy', *Estu. Coast. Shelf Sci.*, under revision (2015).
6. O. Gómez Sichi, Ph. Blondel, E. Gràcia., 'Acoustic textures and seafloor characterisation of submarine landslides – An example from the SW Iberian Margin'. In: Pace N. G. Blondel Ph. (eds), *Boundary Influences in High-Frequency Shallow Water Acoustics*, University of Bath Press (2005).
7. V. Hühnerbach, Ph. Blondel, V.A.I. Huvenne and O. Gómez Sichi., Repeatability of high-resolution sidescan and multibeam backscatter imagery over cold-water corals – possible implications on long-term habitat monitoring, *Proc. Underwater Acoustic Measurements UAM-2007: Heraklion*, 877 (2007).
8. M. Prampolini, Ph. Blondel and F. Foglini., 'Acoustic textures and bathymetry analyses applied to habitat mapping of the Maltese continental shelf', submitted (2015).
9. V.A.I. Huvenne, Ph. Blondel and J.P. Henriët., 'Textural analysis of sidescan sonar imagery from two mound provinces in the Porcupine Seabight' *Mar. Geo.*, 189, 323-341 (2002).
10. Ph. Blondel and O. Gómez Sichi., 'Textural analyses of multibeam sonar imagery from Stanton Banks, Northern Ireland continental shelf', *App. Acous.*, 70(10), 1288-1297 (2009)

11. Ph. Blondel. 'Segmentation of the Mid-Atlantic Ridge south of the Azores, based on acoustic classification of TOBI data'. In: MacLeod, C. J., Tyler, P. A., Walker, C. L. (eds), Tectonic, Magmatic, Hydrothermal and Biological Segmentation of Mid-Ocean Ridges, *Geological Society, London, Special Publications*, 118, 17-28 (1996)
12. Ph. Blondel., 'Automatic mine detection by textural analysis of COTS sidescan sonar imagery', *Int. J. Rem. Sensing*, 21(16), 3115-3128 (2000)